Coalescence kinetics of bare and hydrogen-coated silicon nanoparticles: A molecular dynamics study

T. Hawa and M. R. Zachariah*
Departments of Mechanical Engineering and Chemistry, University of Maryland, College Park, Maryland 20742, USA and the National Institute of Standards and Technology, Gaithersburg, Maryland 20899, USA
(Received 18 May 2004; published 27 April 2005)

One of the significant challenges in the use of nanoparticles is the control of primary particle size and extent of agglomeration when grown from the gas phase. In this paper we consider the role of surface passivation of the rate of nanoparticle coalescence. We have studied the coalescence of bare and H-coated silicon nanoparticles of sizes between 2–6 nm using molecular dynamics simulation at 1000 and 1500 K. We found that coalescence of coated particles consists of two steps, where reaction between particles and relocations of surface atoms near the reacting region, occur in the first step, which comprise an induction period. The second step consists of the nominal coalescence event, which depends on the surface tension and solid-state diffusion in the particle. The hydrogen passivation layer was found to remain on the surface of coalescing pair of the particles during the entire coalescence event. We also develop a mathematical model to describe the dynamics of coalescence of coated particles. The model is able to describe both the initial induction period and the coalescence period, and the role of the extent of surface coverage on the coalescence rate. In general, the entire coalescence time of coated particles is about 3–5 times that of bare particles, and the exothermicity from coalescence is about half that for the unpassivated particles.

DOI: 10.1103/PhysRevB.71.165434 PACS number(s): 61.46.+w, 61.20.Ja

I. INTRODUCTION

Nanoparticles and nanocrystals are considered one of the fundamental building blocks for the creation of nanostructures and associated devices. In particular, for optoelectronic application quantum confinement effects and the role of surface states for particles smaller than 10 nm are of particular interest.[1–4] Fabrication of the desired size with a narrow size distribution, and desired structure, are seen as one of the major challenges in robust implementation of nanoscience to a nanotechnology.

The growth of silicon nanoparticles is usually achieved by gas-phase processes through either thermal decomposition of chemical precursors or some type of physical evaporation and/or condensation process. For example, laser ablation of Si targets in an inert gas have been used successfully to fabricate sub-10 nm Si nanoparticles,[5,6] and are shown to exhibit visible photoluminescence (PL) in the red. However, stable and intense PL in the green-blue region has not been achieved for pure Si nanoparticles because of the nature of surface states arising from dangling bonds.[7–9] Patrone *et al.*, for example, found that PL can be stabilized for deposited Si nanoparticles prepared in a hydrogen-containing atmosphere,[6] and hydrogenated Si nanoparticles with green PL in the gas phase can be fabricated in a H_2+Ne background gas.[10] Makimura *et al.*[10] reported that hydrogen termination of Si nanoparticles surfaces might arrest the growth of particles and/or change the structure. Such Si nanoparticles were shown to have a larger band gap and hence require higher photon energy to realize photoexcitation for PL.[11]

Controlling particle size is also a major challenge in the formation of nanoparticles. Liquid-phase growth methods have received some success in this regard through the use of colloidal and solvation forces, to retard or control cluster-cluster interactions, and therefore the growth of nanoparticles.[1,12] In contrast gas-phase growth, which is a considerably more important industrial process at the moment, has no easy solution to significantly retard particle coagulation and/or coalescence. One possibility has been to charge particles, although this process is difficult to achieve on a large scale, particularly for small particles where charging rates are very small.

A more formal representation of the problem is that the rate of collision and subsequent coalescence of particles determines the size of the spherical primary particles and the growth of agglomerates. When the characteristic coalescence time is less than the collision time between particles (at sufficiently higher temperatures), spherical particles will be produced before another collision event occurs. On the other hand, when the collision time is less than the characteristic coalescence time (at relatively low temperatures), coalescence will be negligibly slow and chain aggregates will be formed,

$$\tau_{\text{coalescence}} < \tau_{\text{collision}} \rightarrow \text{spherical particle},$$

$$\tau_{\text{coalescence}} > \tau_{\text{collision}} \rightarrow \text{agglomerate}.$$

Therefore, particle morphology and size can be controlled by either modifying the characteristic coalescence time or the collision time. We have investigated various experimental and theoretical strategies to accomplish this. By embedding a nanoparticle in a nanodroplet of molten salt, generated from gas-phase precursors injected into a high-temperature flame, we observed a retardation of growth.[13] This process was subsequently modeled by Efendiev and Zachariah[14,15] using a Monte Carlo method for the simulation that combines both the coagulation of the droplets and the interaction between the embedded nanoparticles. Another approach was to con-

trol the coalescence rate by using the inherent exothermicity of particle coalescence to internally heat the particle and therefore control the growth rate.[16] However, many gas phase processes are not amenable to such approaches.

An altogether different approach is to imagine a particle coated with a material that would prevent or retard particle agglomeration or coalescence. More specifically, for the case of silicon, is a natural passivating agent that has been used previously, although not specifically, for silicon nanoparticles.

Since hydrogenated amorphous silicon (*a*-Si:H) has many technological applications,[17] MD simulations have been employed to investigate the reaction dynamics of atomic hydrogen with *a*-Si:H surfaces[18] and H_2 adsorption and desorption on silicon surfaces.[19,20] Moreover, the effect of the radical energization on radical diffusion on a substrate was studied by impinging SiH_3 radicals (a likely precursor for Si growth), to *a*-Si:H thin film growth.[21–27] Ramalingam *et al.* found that thermal and energetic Si_nH_x ($1<n\leqslant 6; 0 \leqslant x \leqslant 13$) clusters reacted with a probability greater than 85% with crystalline surfaces and with *a*-Si:H. Monte Carlo simulations have also been applied to study *a*-Si:H thin films.[28–30] Experiments have shown that hydrogen atoms terminate surface states (dangling bonds) and stabilize the structure of Si_n clusters ($n=2$–10) (Ref. 31) and that the hydride-coated surface prevents the oxygen passivation of the surface.[32]

The review of the previous experimental and numerical studies on the topic of hydrogen termination of the surface of Si shows that surface passivation might be a very effective strategy to control the growth and morphology of nanoparticles grown from the vapor. More recently we have been exploring the possibility of a passivation layer to retard the growth of nanoparticles. In a molecular dynamics study, Hawa and Zachariah[33] evaluated the particle-particle interaction of hydrogen-surface-terminated silicon nanoparticles for sizes between 200 and 6400 silicon atoms at 300–1800 K. We reported that the presence of hydrogen passivation surface on silicon nanoparticles prevented coalescence between particles under thermal collision conditions. The critical approach energy of particle coalescence was significantly higher than the thermal collision energy, and it was found to increase with increasing particle size but decreased with increasing particle temperature. We also found that both solid and liquid droplets were seen to bounce at thermal energies at the temperature range of our study, and in some cases, "superelastic" collisions were observed, where the rebound kinetic energy of the droplet is higher than the approach energy. Moreover, when particles had only 75% of the available surface sites covered with hydrogen, the critical approach energy was significantly reduced but still required superthermal activation.

The above work leads us to study the effect of surface passivation on the dynamics of particle coalescence. Controlling the particle size is one of the most difficult problems in the formation of nanoparticles, in part because the characteristic coalescence time has a nonlinear dependence on temperature. Furthermore, understanding the dynamics of coalescence of surface passivated particles may be important for controlling the morphology of nanoparticles grown from the vapor. For bare particles of equivalent size the characteristic coalescence time calculated from a solid state diffusion model is written as[34]

$$\tau_f = \frac{3kT_pN}{64\pi\sigma D}, \tag{1}$$

where T_p is the particle temperature, N is the number concentration, D is the diffusion coefficient reported as an Arrhenius function of the temperature, and σ is the surface tension. The coalescence time, which increases as the four thirds power of the number concentration N, is also extensively used for the prediction.[35,36] More recently, the relaxation time for solids was found to increase exponentially as a function of the cluster size.[37] For viscous flow, the coalescence time is given by[38]

$$\tau_f = \frac{\eta d_p}{\sigma}, \tag{2}$$

where d_p is the diameter of the particle and η is the temperature-dependent viscosity. In a prior molecular dynamics (MD) study of the kinetics of growth and coalescence of silicon nanoparticles we found that Eqs. (1) and (2) provide a reasonable quantitative description of nanoparticle coalescence.[39] However, in this study we will need to consider the effect of surface passivation on the coalescence process, and the applicability or modification to models described by Eqs. (1) and (2).

In the above relations [Eqs. (1) and (2)] surface tension and atomic transport (diffusion coefficient) play an important role in coalescence. In our recent study of the effect of hydrogen passivation surface on the surface tension and on the diffusion coefficient of the silicon nanoparticles by MD simulation, we found that the surface tension of perfectly coated particles was about a half that of bare particles, but that the diffusion coefficient increased by only about 10% with hydrogen coating.[40] The particle pressure with hydrogen coating was also reduced due to the decrease of the surface tension. Moreover, the surface tension did not depend on particle size. Recent geometric optimizations and MD simulations based on an empirical tight-binding approach for studying the structure of fully and partially hydrogenated Si nanocrystals also showed that the structural properties have little size effect, contrary to their electronic properties,[41] and their results are in agreement with the x-ray diffraction measurements.[42]

From a practical point of view it is well known that silicon particles grown from silane contain significant amounts of hydrogen.[43,44] As we mentioned earlier, the pulsed laser ablation technique is used to generate hydrogenated silicon nanoparticles. It is therefore quite conceivable that one could produce such materials from the vapor with a surface coating of hydrogen near saturation.

The work in this paper is focused on understanding the coalescence mechanisms of surface-coated nanoparticles. We present a mathematical model of surface-coated particles coalescence based on an extension of Frenkel's model.[38] We will also use MD simulations with a reparametrized KTS potential[33] to track the evolution of a coalescence process

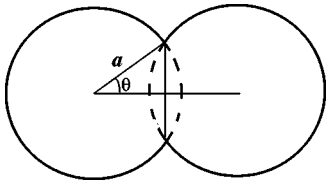

FIG. 1. Geometric representation of the coalescence of the two spherical drops.

and obtain the characteristic coalescence time. We clarify the relationship between the dynamics of the coalescence and the surface tension of the particles, and provide insight into the relationship between the mathematical model and the MD simulation results, and identify the mechanism of surface passivated particle coalescence.

II. MATHEMATICAL MODEL FOR PARTICLE COALESCENCE

Following Frenkel's mathematical analysis,[38] we consider the coalescence of two liquid drops, which are initially in contact with each other at a single point. We also assume that the remaining parts of the two drops maintain a spherical shape (see Fig. 1). Under this condition the distance between the centers of each drop are equal to $2a\cos\theta$, where a denotes the radius of the spherical portion of the drops. From conservation of mass of each drop, the relationship between the radius a, as well as the total surface of the coalescing particles at any time t and at $t=0$, can be obtained (see Frenkel). Figure 2 shows the radius a as a function of θ. Since a does not change significantly when $0<\theta<30°$, we assume that $a\cong a_0$ for small angle of θ. Then, the change of the surface area ΔS can be obtained as

$$\Delta S = 4\pi a_0^2\left[\Delta\theta(-\sin\theta) + \Delta\theta^2\left(-\frac{\cos\theta}{2}\right)\right], \tag{3}$$

where $\Delta\theta \ll 1$. Note that Frenkel considered the second order term dominates the sintering process, but this is true when $\theta=0$. However, the first order term is always larger when $\theta > \Delta\theta$. Moreover, according to Fig. 2, the assumption $a\cong a_0$ can be applied to small θ. Thus, we consider the first order term for the sintering process and neglect the second order term in our analysis.

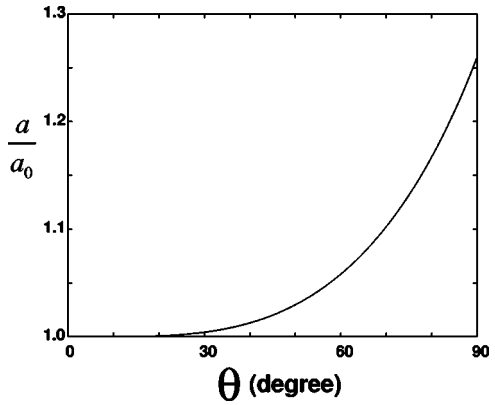

FIG. 2. The radius a as a function of θ.

The internal energy, due to the change in surface area S, is related to the surface tension, such that the rate of energy change during the coalescence of two drops can be expressed as

$$-\sigma\frac{dS}{dt} = -4\pi a_0^2\sigma\left(\sin\theta\frac{d\theta}{dt}\right), \tag{4}$$

where σ denotes the surface tension of the drop. Equation (4) must balance with the rate of energy dissipation due to the viscous flow of the liquid. The extent of this flow can be specified by the decrease of the distance between the center of each drop, and the surface of contact with the other drop. The velocity can be obtained as

$$v = \frac{a_0\cos\theta - a_0\cos(\theta+\Delta\theta)}{\Delta t} \approx a_0\sin\theta\frac{d\theta}{dt}. \tag{5}$$

The velocity gradient γ can be defined, accordingly, as v/a. Under such conditions the energy dissipated in the whole body per unit time is equal, approximately, to[38]

$$2\eta\int_0^{a_0}\gamma^2 2(4\pi r^2)dr = \frac{16}{3}\pi a_0^3\eta\left(\sin\theta\frac{d\theta}{dt}\right)^2, \tag{6}$$

where η is the viscosity.

In our study, we need to consider the effect of surface passivation (hydrogen) on the coalescence process. We assume that the rate of energy of both repulsion, between hydrogen's, and relocation of hydrogen atoms due to the decrease of the surface area is expressed as

$$4\pi a_0^2\beta\xi(\theta)\left(\sin\theta\frac{d\theta}{dt}\right), \tag{7}$$

where β is a positive parameter in energy per unit area and ξ is a nondimensional function of θ. We assume that the parameter β is a linear combination of the effect of the repulsion β_{rep} and the relocation β_{rel} of the surface atoms, and that they are a function of the amount of hydrogen atoms on the surface. We note that pure silicon particles would attract each other, while the hydrogen monolayer creates repulsive forces between the particles. The effective reaction contact area made by an interaction of two spherical particles of the same size is schematically shown in Fig. 3 and given by

$$\pi a(f_c + a\sin^2\theta), \tag{8}$$

where f_c is a cutoff length of the surface atoms obtained by the reparametrized KTS potential[33] mentioned in a later section. The first term is the surface of the sector of the spherical particle obtained from the cutoff length, and the second term is the surface of contact with the other drop. Since the hydrogen monolayer exists only on the surface of the spherical particles, the portion of the reactive contact area covered by the hydrogen monolayer is determined by

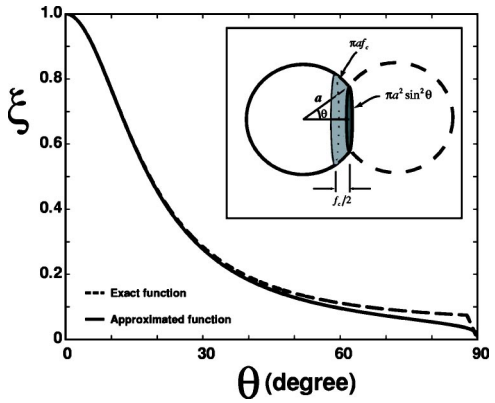

FIG. 3. ξ as a function of θ with the sketch of the effective reaction contact area. An exact and an approximated ξ are described with dashed and solid lines.

$$\xi_{\mathrm{Exact}}(\theta) = 1 \Big/ \left(1 + \frac{a}{f_c}\sin^2\theta\right) \quad \text{for } 0 \leqslant \theta \leqslant 87.7^\circ$$
$$= 1 \Big/ \left(1 + \frac{\sin^2\theta}{2\cos\theta}\right) \quad \text{for } 87.7^\circ < \theta < 90^\circ . \tag{9}$$

Note that near 90° there is a rapid decrease of the reactive surface area of the spherical particle. Figure 3 also shows ξ_{Exact} as a dashed line when the ratio of a/f_c is 10. The approximated expression of ξ is

$$\xi_{\mathrm{Approx}}(\theta) = 1 \Big/ \left(1 + \frac{a}{f_c}\frac{\sin^2\theta}{\cos^{1/4}\theta}\right). \tag{10}$$

The above expression is described as a solid line in Fig. 3. Note that expression (10) describes the dashed line well when θ is small, and that our analysis is limited for small θ. Expression (10) indicates that when θ is small (initial period of coalescence process) a large amount of work is needed for particle reaction against the hydrogen passivation surface and for particle coalescence to relocate the surface atoms. However, after the initial stage of coalescence, the work for relocation of hydrogen atoms quickly decays and disappears when θ is $\pi/2$.

Equating expressions (6) and (7) to (4), we obtain the following equation:

$$\tfrac{16}{3}\pi a_0^3 \eta \gamma^2 + 4\pi a_0^2 \beta \xi(\theta)\gamma = 4\pi a_0^2 \sigma \gamma. \tag{11}$$

Integrating over the entire process of the coalescence, which is $0 \leqslant \theta \leqslant \pi/2$, gives

$$t = \frac{4}{3} a_0 \eta \int_0^{\pi/2} \frac{\sin\theta}{\sigma - \beta\xi(\theta)} d\theta. \tag{12}$$

It is clearly seen that the product $\beta\xi(\theta)$ must be less than the surface tension σ. Thus, $0 \leqslant \beta < \sigma$. Note that the model implicitly neglects the initial approaching energy of the coalescing particles. The justification of the latter point is based on the MD simulations (to be presented later in the text), that under constant temperature processes, the collision energy has a negligible after the initial contact of coalescing particles. The parameter β is zero when there is no surface passivation layer on the particles. In such a case, the time of complete coalescence becomes

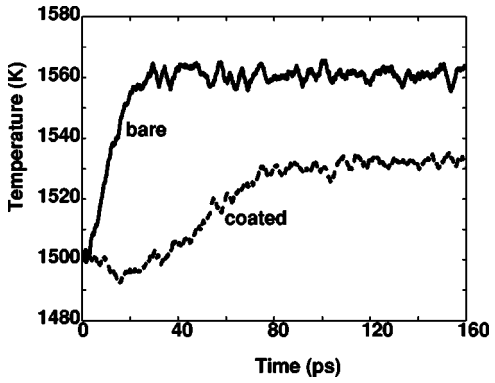

FIG. 4. Temperature evolution during sintering for bare and coated 6 nm particles initially at 1500 K.

$$t = \frac{4}{3}\frac{a_0 \eta}{\sigma}, \tag{13}$$

and is similar expression to the result obtained by Frenkel.[38]

III. COMPUTATIONAL MODEL AND SIMULATION PROCEDURE

This study also involves atomistic simulations using classical molecular dynamics. For this work we use the reparametrized KTS interatomic potential for the silicon-hydrogen system developed by Hawa and Zachariah (HZ).[33] This interatomic potential for silicon was developed by Stillinger and Weber (SW) (Ref. 45) and extended by Kohen *et al.*[46] to include Si-H and H-H interactions. Similar sets of potential energy functions have also been developed by Murty and Atwater,[47] Ohira *et al.*,[23,24,26] and Ramalingam *et al.*[48] where a Tersoff-type potential[49–52] was extended to describe interatomic interactions in the Si:H system. This extended version of the Tersoff potential has been tested successfully for its accuracy in describing the Si:H system in several earlier studies; however, the simulation of liquid silicon was not well described by the potential.[49] By contrast, the extended SW potential (HZ) was designed to describe interactions in both solid and liquid forms of silicon. Since most synthesis processes leading to cluster formation occur at high temperature, cluster growth by coalescence is dominated by liquid-like characteristics, and the accuracy of the SW potential increases with increasing particle size or temperature, we use this potential for our investigations. The HZ potential energy is a sum of two- and three-body interactions, and the details of the model and its parameters are given in the literature (Hawa and Zachariah).[33]

All simulations were run either on an Origin or Cray T3E computer running up to 64 processors. Atom trajectories were determined by integrating the classical equations of motion using the velocity form of the Verlet algorithm,[53] with rescaling of atomic velocities at each time step to achieve temperature control for constant temperature simula-

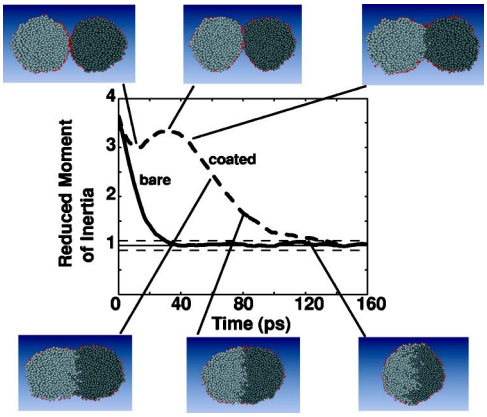

FIG. 5. (Color online) Temporal snapshots of the morphology during sintering of coated 6 nm particles. Inset graphs show the temporal behavior of the reduced moments of inertia for coated and bare particles.

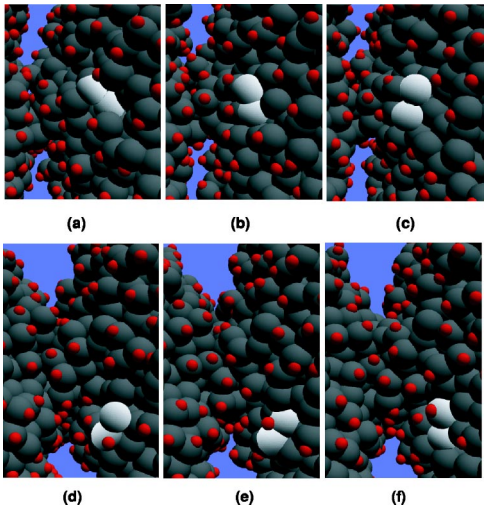

FIG. 6. (Color online) Temporal evolution of the atomic behavior near the initial contact region showing hydrogen hopping and the movement of bare silicon to the surface.

tions. Time steps of 0.5 and 0.05 fs were typically used for pure silicon clusters and for hydrogen-coated clusters, respectively, to ensure energy conservation, and the Verlet neighbor list with parallel architecture was employed in all the simulations, with a neighbor list renewal every 10 steps. The simulations take place in a spherical cavity of 20 nm radius using an elastic boundary condition.

The first step in the equilibration process was to prepare pure silicon particles of various sizes (2, 3, 4, and 6 nm) (200, 800, 1600, and 6400 Si atoms) at 300 K. After removal of angular momentum, the particle temperature was raised to 2100 K for 1 ns. Particle temperatures were then reduced slowly to 300 K and equilibrated for 50 ps. The next step was to coat the particles with hydrogen atoms. Since the particles were already equilibrated, almost all surface atoms had a coordination number of three. A hydrogen atom was placed on each surface silicon atoms at a distance of 1.5 Å, and the particle temperature was maintained at 300 K for 10 ps. Any hydrogen atoms that were released from the surface were removed from the simulation, and the dynamics repeated for 10 ps. As a result, the numbers of hydrogens placed on the silicon particles made of 200, 800, 1600, and 6400 Si atoms are 74, 211, 367, and 785. For preparation of partially hydrogen coated particles, appropriate number of hydrogens were randomly removed from the particles, and again, the dynamics repeated for 10 ps for equilibration. After generating the hydrogen monolayer on the silicon particles, the temperature of the particles was slowly raised to the desired temperatures of 1000 and 1500 K and maintained at constant temperature for 50 ps. For the last step in the preparation process, the simulations were switched to a constant energy calculation for 20 ps. If the average temperature of the particle deviated by more than 10 K over this period, the equilibration process was repeated until the particle temperature deviated by less than 10 K. Duplicated particles were generated and then collided with critical collision energies for adhesion (not static coalescence) found in Hawa and Zachariah.[33]

IV. RESULTS AND DISCUSSION

A. Fully coated vs bare particles

During the coalescence of two particles, the formation of new chemical bonds between the atoms decreases the potential energy of the system, and decreases the total surface area. For two isolated particles under the adiabatic conditions, as the total energy is conserved, the decrease in potential energy causes a rise in thermal motion of atoms in the particle, which is reflected as an increase in particle temperature.[39] Figure 4 shows the temperature change during the coalescence of two 6 nm bare, and fully coated particles in a constant energy simulation. In this case particles have an initial temperature of 1500 K and are then given an additional directional velocity so that they collide with a kinetic energy of 110 000 K. The high collision energy is based on our prior study of the critical collision energy for reaction between fully coated silicon particles.[33] It should be understood that the collision energy is small compared with the total energy of the system, and does not have a significant contribution in the observed temperature rise. It can be seen from Fig. 4 that the uncoated particles show a rapid temperature rise during the first 20 ps (rise of temperature by 60 K), resulting from the energy release during new bond formation. On the other hand, the temperature of the coated particles does not change, but goes through an induction period, for the first 30 ps. It then increases slowly by 30 K, which is about a half the temperature rise as compared to the bare particle coalescence case. This difference in temperature is a consequence of formation of 379 vs 183 new bonds in bare and fully coated particles, respectively. This may be an indication of change of the particle structure due to the hydrogen coating and will be discussed in detail later in the manuscript.

The corresponding structural dynamics can be studied from the temporal variation of the reduced moment of inertia in the direction of collision and particle morphology, as shown in Fig. 5. The reduced moment of inertia converges to

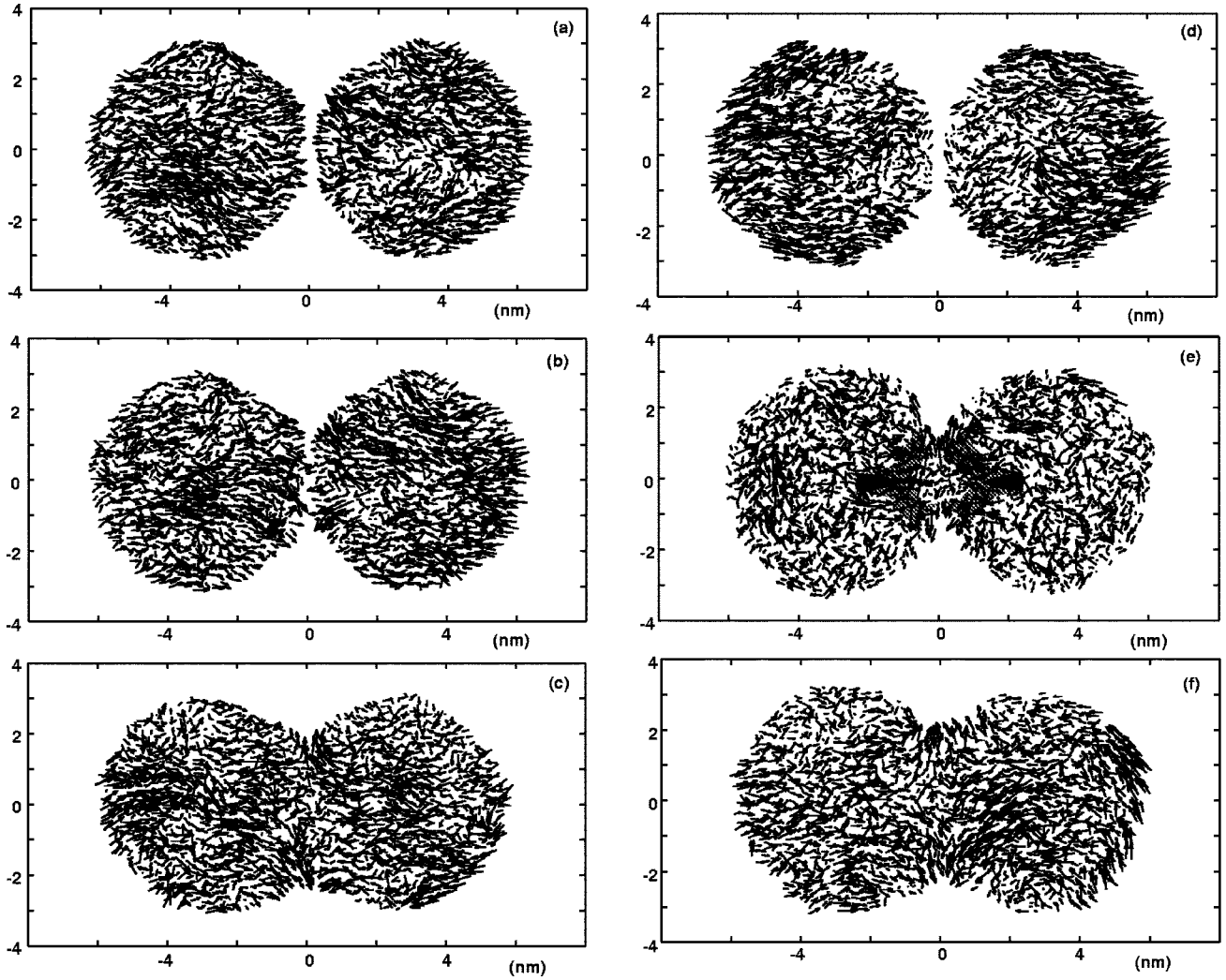

FIG. 7. Time series of particle morphology imaged with respect to atomic velocity vectors for two 6 nm particles at 1500 K. (a), (b), and (c) are bare and (d), (e), and (f) are coated particles.

unity when the particle is spherical. However, as these particles (2–6 nm) are under constant movement due to the atomic motion, they would never become perfectly spherical. Therefore, we define a reduced moment of inertia of 1.1 as the condition for achieving complete coalescence. It can be seen that for the case of bare silicon particles, the reduced moment of inertia converges to 1.1 (spherical shape) monotonically. For the bare particles, the interparticle interaction due to the surface atoms is attractive and there is no need to provide a potential energy barrier to induce the reaction. In contrast to this, the fully coated clusters, and as reflected in the temperature rise plot shown in Fig. 4, show an induction period before the reduction in the moment of inertia. In fact, the moment of inertia initially increases after the collision, reaches a maximum, and then subsequently decreases toward unity. In this case the initial interparticle interaction is between the surface hydrogen atoms, and is repulsive.

The initial increase of the moment of inertia is attributed to an increase in total surface area of the coalescing particles. Figure 6 demonstrates the temporal evolution of the atomic behavior near the initial contact surface. The small light gray and large dark gray spheres represent H and Si atoms in the figure. Two Si atoms colored white are initially beneath the surface of the coalescing particle [Fig. 6(a)], as coalescence begins, one of the white atoms comes to the surface [Fig. 6(b)]. A second one follows the first and stretches the surface and leaves a bare silicon surface [Fig. 6(c)]. We note that rather than a Si-H molecule moving interior to the particle to reduce surface area, bare silicon actually moves to the exterior, and at least initially this is responsible for an initial increase in moment of inertia. At no time do we see H atoms enter the interior of the particle. However, we do observe hopping of H atoms on the surface during the entire coalescence period and the opening of bare silicon spots facilitates this movement. In image 6(d) we see the beginning of this migration process where a white Si (bare) atom and a hydrogenated neighbor experience a hydrogen exchange. In Fig. 6(e) we see that the previously hydrogenated Si is pulled out of the surface, and donates its hydrogen to the neighboring white Si atom [Fig. 6(f)]. These events suggest that the mathematical model for the coalescence of coated particles needs to account for the relocation of surface atoms.

To better understand the nature of the evolution in the morphology, we study the properties of both bare and coated

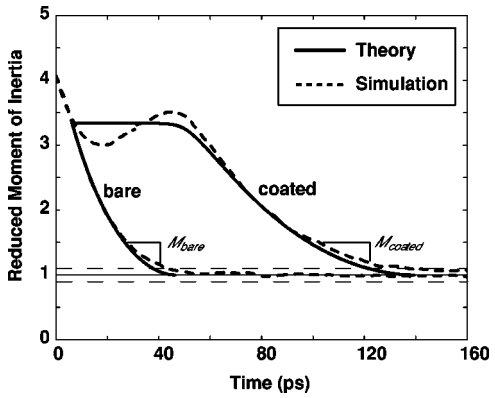

FIG. 8. Temporal behavior of the reduced moment of inertia for bare and coated 6 nm particles during a constant temperature (1500 K) coalescence process. Solid lines, model; dashed line, MD simulation.

particles in detail. The change in morphology of the clusters could be through movement of atoms via bulk fluid motion or by individual atomic diffusion processes. Figure 7 demonstrates the temporal evolution of the atomic velocity vectors, shown as a cross section slice of thickness -0.5 nm $< y < 0.5$ nm, during a coalescence event of bare and coated particles. As the bare particles approach, surface atoms are accelerated toward each other, as they feel an attractive force [Fig. 7(a)], which continues even after the collision [Fig. 7(b)]. Once the collision event has progressed, diffusion processes drive the agglomerate to become a sphere [Fig. 7(c)]. On the other hand, as the fully coated particles approach, the surface hydrogen atoms feel a repulsive force [Fig. 7(d)]. After reaction, the surface atoms in the contact area move away from the neck of the agglomerate, while interior (core) atoms move toward the neck [Fig. 7(e)]. This is schematically illustrated by the large arrows showing the net direction of atom movement. The surface atoms being squeezed out of the neck region, move along with the surface of the particles. This is manifested by both Si-H diffusion and H hopping. Finally in Fig. 7(f) the incoming interior atoms widens the neck of the agglomerate and drives it to a sphere. According to Fig. 5, the coated particles coalescence process [Figs. 7(d)–7(f)] requires more time than the bare particle coalescence process [Figs. 7(a)–7(c)]. After the process 7(d)–7(f), the reduced moment of inertia monotonically converges to unity, and the temporal evolution of particle morphology is very similar to that seen for bare particles.

During the coalescence process, temperature change of clusters affects properties such as diffusivity and complicates the calculation of characteristic coalescence time from Eqs. (1), (2), and (12). In order to simplify this problem we chose to study the coalescence process under constant temperature conditions. In point of fact for a real growth process, particles of this size would not see temperature excursions, since they are effectively thermostated by surrounding gas.[16] The molecular dynamics simulation of the reduced moment of inertia for both bare and fully coated 6 nm particles at 1500 K shown as dashed lines are presented in Fig. 8, and are similar in form to that seen in Fig. 5. A direct observation of the two curves shows that the decay toward spherical shape is similar once the initial induction period for the coated particles is accounted for. Temporal variations of the total surface area of coalescing particles obtained from our mathematical model (3), (10), and (12) are compared with the simulation results for both bare as well as coated cases. The radius a of 3 nm and the cutoff length f_c of 0.3 nm were chosen, to give the function $\xi(\theta)$ shown in Fig. 3. The parameter β of 0.441 J/m^2 was chosen to fit the molecular dynamics results. Note that our model does not describe the behavior of the initial variation of the moment of inertia of the coated particles, because of the assumption of spherical shape during coalescence. However, the model predicts the initial induction period by adjusting the parameter β. According to our discussion in the previous section, this induction period occurs due to (a) diffusion of surface atoms along the particle surface, (b) movement of interior Si atoms near the surface toward the particle surface, and (c) movement of core Si atoms to fill in the neck of the coalescing particles. During the initial contact period, the large magnitude of the function $\xi(\theta)$ retards particle coalescence. Moreover, it is clearly seen that our model not only describes the dynamical behavior of the moment of inertia after the initial induction period, but also shows good agreement with the coalescence time for bare as well as coated particles. Since the function $\xi(\theta)$ decays significantly toward the end of the coalescence process, the characteristic coalescence time for liquid droplets according to expressions (2) and (12) is approximately inversely proportional to the surface tension of the particles. We compare the characteristic coalescence time with the decay rate of the reduced moment of inertia, M. The surface tensions of bare and fully coated particles were taken as 0.826 and 0.442 J/m^2, respectively, as computed by our prior simulations, and the ratio $\sigma_{\text{coated}}/\sigma_{\text{bare}}$, was found to be 0.54.[40] We calculate the time of both bare and coated coalescence processes from the reduced moment of inertia 2.5 to 1.1 in Fig. 8. These periods are 31.2 and 64.0 ps for bare and coated cases, and their ratio is 0.48. We also obtain the ratio of those decay rates observed, M_{bare} and M_{coated}, from Fig. 8, which gives 0.55. Both decay rates, M, are the times required to decrease the reduced moment of inertia from 1.5 to 1.2, where the growing particle is nearly spherical. These ratios clearly indicate excellent agreement with the ratio of the characteristic coalescence times, and those results suggest that once a standard coalescence process [e.g., after the period of Fig. 7(f)] is initiated, the coalescence event between a coated and uncoated are primarily controlled by the same internal transport/kinetic processes, and that the difference in the predicted coalescence time is determined by the differences in surface tension. The deviation between the mathematical model and the simulation results near the end of the coalescence process of both bare and fully coated particles is due to the assumption that particle radius does not change.

B. Size and temperature dependence

The effect of the particle size and the initial particle temperature on the particle coalescence was also studied. Figures 9(a) and 9(b) show the temporal behavior of temperature and reduced moment of inertia for bare and fully coated 3 nm

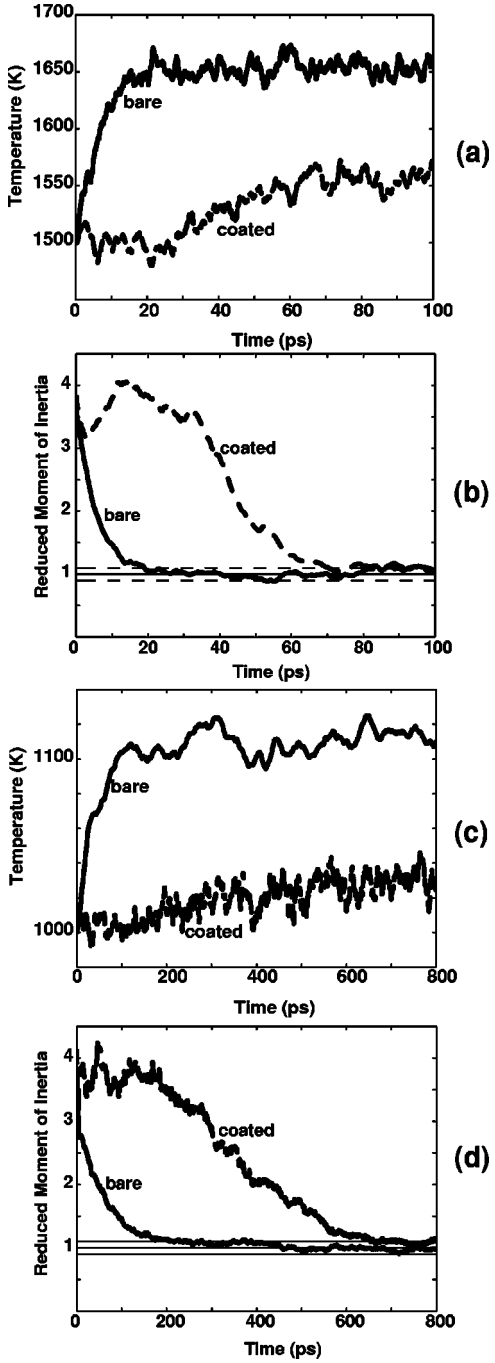

FIG. 9. Temperature and reduced moment of inertia of the coalescing pair for both bare and coated 3 nm particles (a) and (b) 1500 K initial temperature and (c) and (d) 1000 K initial temperature.

particles under an energy conservation coalescence process. The initial particle temperature is 1500 K and the initial approaching kinetic energy of 35 000 K corresponds to the critical approach energy for this particular size and particle temperature.[33] By comparison with the 6 nm particle case, the temperature of bare 3 nm particles after the coalescence is higher than that of 6 nm particles (see also Fig. 4). This results from the smaller particles having a greater fractional increase in the number of new bonds formed, which release heat, and the lower heat capacity of the smaller particles.

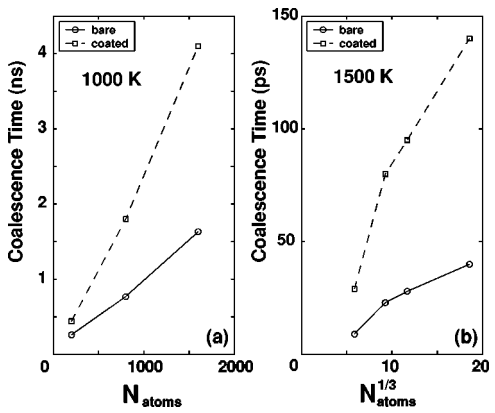

FIG. 10. Coalescence times as a function of particle size (a) 1000 K and (b) 1500 K.

However, the temperature increase of coated coalescing particles is again half that of bare particles, similar to the 6 nm case. Also, the dynamical behavior of temperature and reduced moment of inertia are similar to the coalescence of 6 nm particles. Figure 9(b) shows that the coated particles coalesce a factor of 3.7 times slower than the bare particles and coalescence much faster, about a factor of 2, relative to the corresponding 6 nm particles.

Figures 9(c) and 9(d) show that the temporal variations of temperature and reduced moment of inertia of 3 nm at a lower temperature of 1000 K and an initial approaching kinetic energy is 60 000 K (critical approaching energy for this size and temperature[33]). The behavior is similar to the higher temperature case; however, the coalescence process is considerably slower (by a factor of 10) and therefore so is the temperature rise. The temperature increase of about 100 K is less than the 1500 K case, which is about 150 K [see Fig. 9(a)]. Since the particle sizes are the same, and in both cases coalescence leads to spherical particles, the number of new bonds (89 at 1500 K, 100 at 1000 K) due to the coalescence is comparable to each other. Therefore, the temperature rise is proportional to their initial particle temperatures and also implies that the heat capacity is relatively constant over this temperature range. On the other hand, the temperature of the coated particle increases slowly, and at complete coalescence the temperature rise is only a third that of the bare particle. We discuss the reasons for this effect in the section on the role of extent of hydrogen surface coverage.

Coalescence times simulated under constant temperature processes as a function of particle size at 1000 K (a) and 1500 K (b) are summarized in Fig. 10. Note that the horizontal axes in the figures are presented as the number of atoms at 1000 K and atoms to the one-third power at 1500 K. This reflects the power dependence to atom number in the phenomenological models for solids and liquids, respectively [Eqs. (1) and (2)]. At 1500 K the coalescence times of both bare and coated particles larger than 800 Si atoms (about 3 nm size) increase linearly with the diameter of the particle, in agreement with Eq. (2). Moreover, at 1000 K the coalescence times of both bare and coated particles increase linearly with the volume of the particle suggested in Eq. (1), and is different from the higher power dependence model.[35–37] At this temperature, and based on our prior work[54] particles are in a

solid/liquid transition phase for these particle sizes. One should expect, however, to observe higher power dependences when particle temperatures are even lower; however, because of the considerably slower rate of coalescence such a computation is not tractable with our MD methods. In addition, Xing and Rosner introduced a surface curvature-dependent diffusivity and applied it to the coalescence model.[55] They found that the coalescence times were many orders of magnitude smaller than those obtained from the macroscopic properties. In our simulations in the range of less than 1000 Si atoms at 1500 K, both bare and coated particles show the effect of surface curvature dependence on the coalescence times.

Coalescence times of fully coated particles are longer (about a factor of 3–5) than that of bare particles at both temperatures, and also show a similar particle size dependence as those of bare particles of corresponding temperatures. Under constant temperature processes, we found that the differences in coalescence behavior between bare and fully coated particles were the initial adhesion-coalescence process, and the decay rate of the reduced moment of inertia associated with a change in surface tension. While many macroscopic parameters (temperature, surface tension, etc.) affect particle coalescence, at the microscopic level coalescence is ultimately an atomic diffusion process, and we observe the effect of these macroscopic parameters on atomic diffusion through the sintering process.[56–58] As such we expect coalescence to be self-similar for both bare and coated clusters. The decrease in surface tension implies a great surface atom stability and slows the coalescence of coated particles by retarding diffusion; however, both diffusion mechanisms are similar. The initial adhesion-coalescence process simply delays the coalescence process, but does not alter the nature of the coalescence behavior. Therefore, while the coated particles can significantly retard coalescence, once the initial reaction barrier is overcome, through the critical collision energy, the behavior of the size-dependent coalescence times of coated particles is similar to that of bare particles.

C. Partially coated particles

The effect of surface coverage on the particle coalescence was also studied. We prepared 30% (236 H atoms), 50% (393 H atoms), 60% (471 H atoms), 75% (589 H atoms), and 85% (668 H atoms) coated 6 nm silicon particles at 1500 K, and these particles were then used to study coalescence under constant temperature conditions. The molecular dynamics simulation for the temporal variation of the reduced moment of inertia are presented in Fig. 11 as dashed lines, for bare to fully (100%) coated particles. Clearly, the coalescence time is significantly, but smoothly, a function of hydrogen surface coverage. During the initial induction period, coalescence as measured by the reduction in moment of inertia shown a monotonic decrease with time. However, for particles with surface coverage of 75% or higher, particles experience an induction period as previously described. The moment of inertia decays to a local minimum, before increasing again, followed by a monotonic drop-off as coalescence takes place. We recall that the increase in surface area

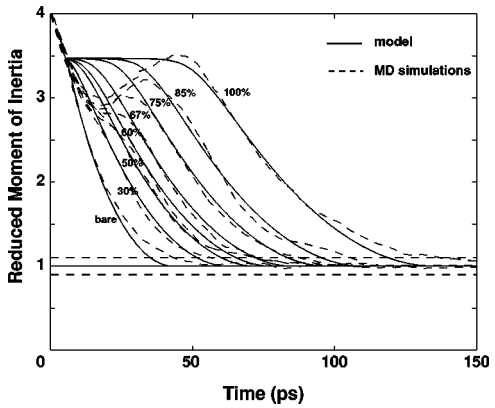

FIG. 11. Reduced moment of inertia of 6 nm particles during sintering for various amounts of hydrogen coverage at 1500 K. Solid line, model; dashed line, MD simulation.

during the induction period results from subsurface silicon atoms coming to the surface. The growth rates from the moment of inertia are qualitatively similar to those of any amount above 75% coating, but the growth periods become longer with increasing surface coverage. Also according to our earlier discussion, the increase of surface area of the coalescing particles is seen as an increase in the moment of inertia. Since the effect of the extent of surface coverage on the Si diffusivity was found to be negligible, the movement of interior Si atoms toward the surface is independent of surface coverage.[40] However, the greater the surface coverage the greater the number of Si atoms that must move to the surface for coalescence to occur. Thus, the transient growth in surface area during the induction period should be proportional to surface coverage. The MD simulation results indicate that the higher the surface coverage, the greater the increase of surface area, and why the induction period increases as the extent of coating increases.

These molecular dynamics results have been compared with the mathematical model (12) shown as solid lines in the same figure. The surface tensions from our previous MD simulations were found to be 0.6394, 0.7548, and 0.8209 J/m^2 for 85, 75, and 50% coated particles, respectively. This conditions corresponded to β's of 0.639385, 0.75475, and 0.80000 J/m^2 as fit the molecular dynamics simulations for the three coverages. As we discussed in the previous section, the nature of our model is such that the initial variation of the moment of inertia cannot be predicted by our model. However, the model successfully describes the initial induction period, and it shows very good agreement with the monotonic decay in the moment of inertia. Note that our model cannot describe the end of the coalescence process because the particle radius a is assumed constant. This comparison indicates that the model predicts the overall process as comprised of an induction period and coalescence period, of any extent of coverage by appropriate choice of β.

We briefly discuss the nature of the β parameter which can be used to determine the initial induction period and the energy requirement for both repulsion and relocation of surface atoms during the initial contact. If one considers that β is a modifier to the surface tension we can define a new parameter $\Gamma=(\sigma-\beta)$, the effective surface tension. Figure 12

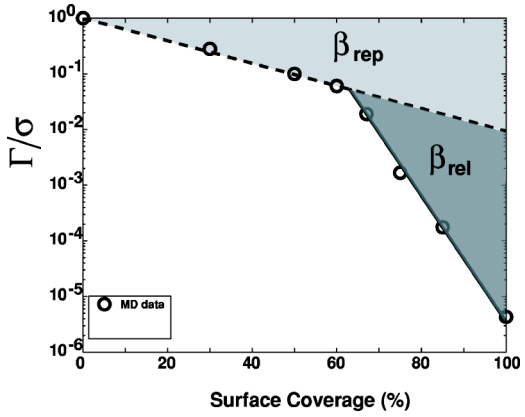

FIG. 12. Relationship between the parameter β and the coverage.

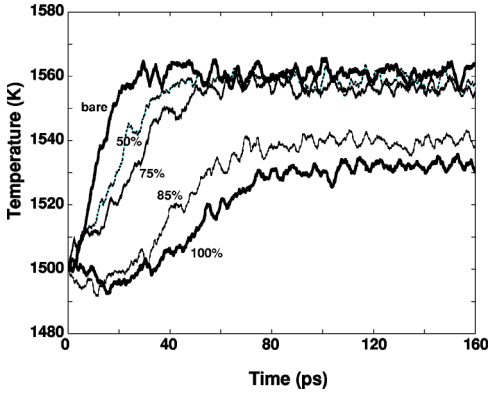

FIG. 13. Temporal behavior of particle temperatures during sintering for various amounts of coating.

shows the effective surface tension normalized by the absolute surface tension as a function of surface coverage. At very low coverage, β is small, and the effective surface tension is near the true surface tension. With increasing coverage, the effective surface tension decreases, making it harder for particles to coalesce.

When the extent of coverage is below 60%, the normalized effective surface tension decays exponentially with the extent of coating. Above about 67%, the normalized effective surface tension decreases even more rapidly. From the previous section, we saw that for bare particles the interparticle interaction between surface atoms is attractive and no potential energy barrier exists to coalescence. In contrast for coated particles, the interparticle interaction is repulsive and increases with increasing hydrogen coverage. The dashed line in the Fig. 12 describes the effect of repulsion, and the corresponding parameter we define as β_{rep} as a function of coverage

$$\beta_{\text{rep}} = \sigma(1 - 699\,450e^{-0.26P_c}) \quad \text{for any } P_c, \tag{14}$$

where P_c is the percent coating. When $P_c \geqslant 67$, we observe an induction period as the time necessary to relocate surface atoms (see Fig. 11). The change in slope seen in Fig. 12 corresponds to the appearance of the induction period and a new parameter $\beta_{\text{rel}} = \beta - \beta_{\text{rep}}$ which corresponds to the energy needed not only the repulsion (dashed line in Fig. 12) but also for relocation of surface hydrogen and silicon atoms (solid line). This effect increases with P_c and causes the parameter β to approach the surface tension rapidly. The parameter β_{rel} corresponding to such a relocation process is given by

$$\beta_{\text{rel}} = \sigma(699\,450e^{-0.26P_c} - e^{-0.0467P_c}) \quad \text{for } P_c \geqslant 67. \tag{15}$$

The parameter β is effectively given as β_{rep} for $P_c \leqslant 60$ and $\beta_{\text{rep}} + \beta_{\text{rel}}$ for $P_c \geqslant 67$.

We have also studied the effect of the extent of coating on the temporal variation of temperature during sintering. The molecular dynamics simulations for various extents of coating were carried out under the constant energy conditions, and the results for particle temperatures shown in Fig. 13. Clearly seen is that all with increasing surface coverage, the temperature rise of this exothermic event is moderated relative to bare particles. This is expected as the temperature rise is associated with the formation in net of new chemical bonds. We see that for particles with coverage of 75% or less the final temperatures of the particles are essentially equivalent. While at higher surface coverage the rise in temperature is tempered.

When two equivalent spherical particles coalesce to form a larger spherical particle, the surface area decreases about 20%. This implies that when hydrogen atoms cover more than 80% of the surface of the initial coalescing particles, there exists an excess amount of hydrogen after the completion of coalescence. Since it was found that the hydrogen atoms always stay on the surface during the entire period of coalescence, the existence of hydrogen modifies the structure of silicon atoms near the surface, and moderates the final temperature of the coated particle. The number of SiH_2 and SiH_3's on the surface of 6 nm particles before and after coalescence were found to increase from 38 to 94 and from 0 to 4 for 100% coated particles during coalescence.

V. CONCLUSION

Classical molecular dynamics simulations using the reparametrized three-body KTS potential were conducted to study the coalescence behavior of hydrogen-terminated silicon nanoparticles. The simulations were carried out over a particle size range of 2–6 nm and at 1000 and 1500 K. It was found that there exist two steps during the coalescence of coated particles. The initial step consists of adhesion of two particles and relocations of surface atoms near the adhesion region. This happens due to the existence of H atoms on the surface of the coalescing pair of coated particles. This initial step requires a relatively longer time as compared to the time required for the completion of the coalescence of bare particles. The last step in coalescence consists of the nominal coalescence similar to that observed during coalescence of bare particles and primarily depends on the surface tension and diffusivity of the particle. A mathematical model has been developed that is able to capture both the induction and coalescence event accurately and can be used in phenomenological models for aerosol dynamics. The coalescence time

of the entire process takes longer with increasing particle size and decreasing initial particle temperature. The total coalescence time of coated particles is about 3 to 5 times longer than that of bare particle and the temperature rise of coated particles was found to be about half of that of the corresponding bare particles. As the particle sinters the numbers of SiH_2 and SiH_3 species on the surface of the particle increase due to the reduction in total surface area and the presence of excess H atoms. We also studied the effect of the extent of H coverage on the particle coalescence process and observed a steady decrease in coalescence time with decreasing hydrogen coverage.

ACKNOWLEDGMENTS

This work is supported by NSF Grant No. CTS-0083062, the Army High Performance Computing Research Center Contract No. DAAD19-01-2-0014, the Minnesota Supercomputer Center, and the National Institute of Standards and Technology.

*Author to whom correspondence should be addressed.

[1] A. P. Alivisatos, Science **271**, 933 (1996).
[2] V. L. Colvin, A. P. Alivisatos, and J. G. Tobin, Phys. Rev. Lett. **66**, 2786 (1991).
[3] A. N. Goldstein, C. M. Echer, and A. P. Alivisatos, Science **256**, 1425 (1992).
[4] J. Shi, S. Gider, K. Babcock, and D. D. Awschalom, Science **271**, 937 (1996).
[5] E. Werwa, A. A. Seraphin, L. A. Chiu, C. Zhou, and K. D. Kolenbrander, Appl. Phys. Lett. **64**, 1821 (1994).
[6] L. Patrone, D. Nelson, V. I. Safarov, S. Giorgio, M. Sentis, and W. Marine, Appl. Phys. A: Mater. Sci. Process. **69**, 217 (1999).
[7] L. Tsybeskov and P. M. Fauchet, Appl. Phys. Lett. **64**, 1983 (1994).
[8] H. Mizuno, H. Koyama, and N. Koshida, Appl. Phys. Lett. **69**, 3779 (1996).
[9] H. Mizuno and N. Koshida, in *Microcrystalline and Nanocrystalline Semiconductors*, edited by L. T. Canham, M. J. Sailor, K. Tanaka, and C. Tsai, MRS Symposia Proceedings No. 536 (Materials Research Society, Pittsburgh, 1999), p. 179.
[10] T. Makimura, T. Mizuta, and K. Murakami, Jpn. J. Appl. Phys., Part 2 **41**, L144 (2002).
[11] Y. Kanemitsu, *Optical Properties of Low-Dimensional Materials* (World Scientific, Singapore, 1995).
[12] C. B. Murray, D. J. Norris, and M. G. Bawendi, J. Am. Chem. Soc. **115**, 8706 (1993).
[13] S. H. Ehrman, S. K. Friedlander, and M. R. Zachariah, J. Aerosol Sci. **29**, 687 (1998).
[14] Y. Efendiev and M. R. Zachariah, Chem. Eng. Sci. **56**, 5763 (2001).
[15] Y. Efendiev and M. R. Zachariah, J. Colloid Interface Sci. **249**, 30 (2002).
[16] D. Mukherjee, C. G. Sonwane, and M. R. Zachariah, J. Chem. Phys. **119**, 3391 (2003).
[17] R. A. Street, *Hydrogenated Amorphous Silicon* (Cambridge University Press, Cambridge, UK, 1991).
[18] P. Kratzer, J. Chem. Phys. **106**, 6752 (1997).
[19] P. Kratzer, B. Hammer, and J. K. Norskov, Phys. Rev. B **51**, 13 432 (1995).
[20] P. Kratzer, E. Pehlke, M. Scheffler, M. B. Raschke, and U. Hofer, Phys. Rev. Lett. **81**, 5596 (1998).
[21] F. R. Jeffery, H. R. Shanks, and G. C. Danielson, J. Appl. Phys. **50**, 7034 (1979).
[22] N. Itabashi, N. Nishiwaki, M. Magane, S. Naito, T. Goto, A. Matsuda, C. Yamada, and E. Hirota, Jpn. J. Appl. Phys., Part 1 **29**, L505 (1990).
[23] T. Ohira, T. Inamuro, and T. Adachi, in *Amorphous Silicon Technology*, edited by E. A. Schiff, M. Hack, A. Madan, M. Powell, and A. Matsuda, MRS Symposia Proceedings No. 336 (Materials Research Society, Pittsburgh, 1994), p. 177.
[24] T. Ohira, O. Ukai, T. Adachi, Y. Takeuchi, and M. Murata, Phys. Rev. B **52**, 8283 (1995).
[25] T. Ohira, O. Ukai, M. Noda, Y. Takeuchi, M. Murata, and H. Yoshida, in *Materials Theory, Simulations, and Parallel Algorithms*, edited by E. Kaxiras, J. Joannopoulos, P. Vashishta, and R. K. Kalia, MRS Symposia Proceedings No. 408 (Materials Research Society, Pittsburgh, 1996), p. 445.
[26] T. Ohira, O. Ukai, and M. Noda, Surf. Sci. **458**, 216 (2000).
[27] S. Ramalingam, D. Maroudas, and E. S. Aydil, J. Appl. Phys. **84**, 3895 (1998).
[28] K. K. Gleason, K. S. Wang, M. K. Chen, and J. A. Reimer, J. Appl. Phys. **61**, 2866 (1987).
[29] M. J. McCaughey and M. J. Kushner, J. Appl. Phys. **65**, 186 (1989).
[30] D. W. Brenner, D. H. Roberson, R. J. Carty, D. Srivastava, and B. J. Garrison, in *Computational Methods in Materials Science*, edited by J. E. Mark, M. E. Glicksman, and S. P. Marsh, MRS Symposia Proceedings No. 278 (Materials Research Society, Pittsburgh, 1992), p. 255.
[31] M. O. Watanabe, H. Murakami, T. Miyazaki, and T. Kanayama, Appl. Phys. Lett. **71**, 1207 (1997).
[32] R. L. Mills, B. Dhandapani, and J. He, Sol. Energy Mater. Sol. Cells **80**, 1 (2003).
[33] T. Hawa and M. R. Zachariah, Phys. Rev. B **69**, 035417 (2004).
[34] S. K. Friedlander and M. K. Wu, Phys. Rev. B **49**, 3622 (1994).
[35] C. Herring, Phys. Rev. **82**, 87 (1951).
[36] F. A. Nichols and W. W. Mullins, J. Appl. Phys. **36**, 1826 (1965).
[37] N. Combe, P. Jensen, and A. Pimpinelli, Phys. Rev. Lett. **85**, 110 (2000).
[38] J. Frenkel, J. Phys. (Moscow) **9**, 385 (1945).
[39] M. R. Zachariah and M. J. Carrier, J. Aerosol Sci. **30**, 1139 (1999).
[40] T. Hawa and M. R. Zachariah, J. Chem. Phys. **121**, 9043 (2004).
[41] D. K. Yu, R. Q. Zhang, and S. T. Lee, J. Appl. Phys. **92**, 7453 (2002).
[42] D. Bellet, G. Dolino, M. Ligeon, P. Blanc, and M. Krisch, J. Appl. Phys. **71**, 145 (1992).
[43] A. A. Onischuk, V. P. Strunin, M. A. Ushakova, and V. N. Panfilov, Phys. Status Solidi B **186**, 43 (1994).
[44] A. A. Onischuk, V. P. Strunin, M. A. Ushakova, R. I. Samoilova, and V. N. Panfilov, Phys. Status Solidi B **193**, 25 (1996).
[45] F. H. Stillinger and T. S. Weber, Phys. Rev. B **31**, 5262 (1985).
[46] D. Kohen, J. C. Tully, and F. H. Stillinger, Surf. Sci. **397**, 225 (1998).

[47] M. V. R. Murty and H. A. Atwater, Phys. Rev. B **51**, 4889 (1995).
[48] S. Ramalingam, D. Maroudas, and E. S. Aydil, J. Appl. Phys. **84**, 3895 (1998).
[49] J. Tersoff, Phys. Rev. B **38**, 9902 (1988).
[50] J. Tersoff, Phys. Rev. Lett. **56**, 632 (1986).
[51] J. Tersoff, Phys. Rev. B **37**, 6991 (1988).
[52] J. Tersoff, Phys. Rev. B **39**, 5566 (1989).
[53] L. Verlet, Phys. Rev. **159**, 98 (1967).
[54] M. R. Zachariah and M. J. Carrier, J. Aerosol Sci. **30**, 1139 (1999).
[55] Y. Xing and D. E. Rosner, J. Nanopart. Res. **1**, 277 (1999).
[56] M. R. Zachariah, M. J. Carrier, and E. Blaisten-Barojas, in *Molecularly Designed Ultrafine/Nanostructured Materials*, edited by K. E. Gonsalves, G-M. Chow, T. D. Xiao, and R. C. Cammarata, MRS Symposia Proceedings No. 351 (Materials Research Society, Pittsburgh, 1994), p. 343.
[57] M. Kusunoki, K. Yonimitsu, Y. Sasaki, and Y. Kubo, J. Am. Ceram. Soc. **76**, 763 (1993).
[58] J. E. Bonevich and L. D. Marks, J. Mater. Res. **7**, 1489 (1992).